Supplementary Information

Solid-state graphene formation via nickel carbide intermediate phase

W. Xiong,[a] Y. S. Zhou, [a] W. J. Hou,[a] T. Guillemet,[a,b] J. F. Silvain,[a,b] Y. Gao,[a] M. Lahaye,[b] E. Lebraud,[b] S. Xu,[c] X. W. Wang,[c] D. A. Cullen,[d] K. L. More,[d] L. Jiang,[e] and Y. F. Lu*[a]

[a]Department of Electrical Engineering, University of Nebraska-Lincoln, Lincoln NE 68588, USA.

[b]Institut de Chimie de la Matière Condensée de Bordeaux, Avenue du Docteur Albert Schweitzer F-33608 Pessac Cedex, France.

[c]Department of Mechanical Engineering, Iowa State University, Ames, IA 50011, USA.

[d]Materials Science & Technology Division, Oak Ridge National Laboratory, Oak Ridge, TN 37831, USA.

[e]Laser Micro/Nano Fabrication Laboratory, School of Mechanical Engineering, Beijing Institute of Technology, Beijing 100081, China.

*Corresponding Author: ylu2@unl.edu

1. TEM characterization of graphene and Ni_3C phase from RTP process.
2. Dependence of graphene quality on RTP heating rate.
3. Dependence of graphene quality on RTP heating temperature.
4. Theoretical calculation of Ni_3C decomposition temperature and carbon diffusion length as functions of RTP heating rate.
5. Weight loss measurements in RTP process.
6. Auger electron spectroscopy (AES) spectra of compositional elements.

1. TEM characterization of graphene and Ni_3C phase from RTP process

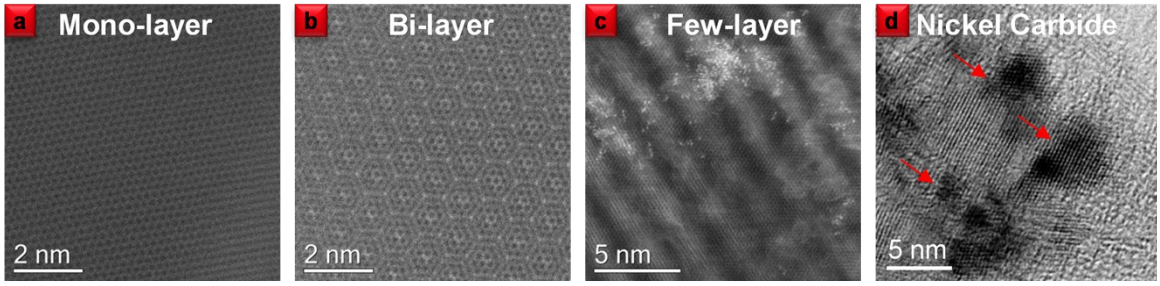

Fig. S1. High resolution TEM characterization of graphene and nickel carbide. (a) mono-layer graphene, (b) bi-layer graphene, (c) few-layer graphene and (d) nickel carbide obtained from the RTP annealing process.

Fig. S1 shows high resolution, medium-angle annular dark field STEM images of the graphene grown from RTP processes. Mono-layer, bi-layer and few-layer graphene were all characterized and observed. The intermediate phase of Ni_3C in the RTP heating processes was also observed in the bright-field TEM image, as shown by the arrows in Fig. S1d.

2. Dependence of graphene quality on the RTP heating rate

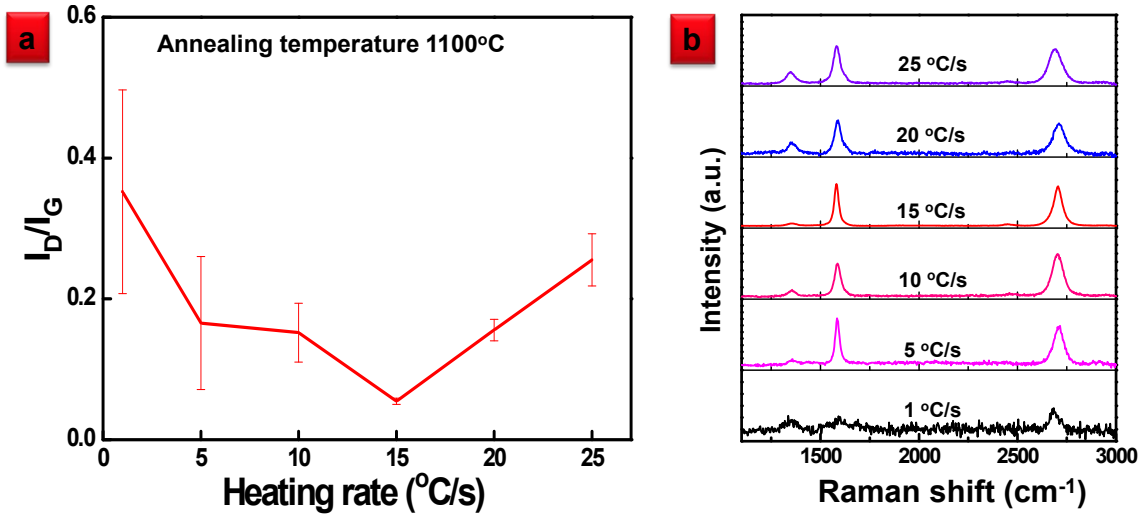

Fig. S2. Dependence of graphene quality on the RTP heating rate when the annealing temperature is set at 1100 °C. (a) I_D/I_G ratio plot as a function of heating rate. (b) Corresponding Raman spectra under different heating rates.

Fig. S2 shows the dependence of graphene quality on the heating rate when the annealing temperature is set at 1100 °C. At the low heating speed of 1 °C/s, the Raman spectrum shows

a high I_D/I_G ratio which indicates the as-formed graphitic layer under this condition has a high level of lattice defects. As the heating rate increases, the I_D/I_G ratio decreases, suggesting improved graphene quality. However, when the heating rate increases above 15 °C/s, the I_D/I_G begins to increase indicating increased defects. Fig. S2 shows that the optimal heating rate for high-quality graphene growth is around 15 °C/s with an annealing temperature of 1100 °C.

3. Dependence of graphene quality on the RTP annealing temperature

Fig. S3 shows the dependence of graphene quality (represented by I_D/I_G ratio) on the RTP annealing temperature with a heating rate of 15 °C/s. The I_D/I_G ratio decreases as the RTP annealing temperature increases, indicating improved graphene quality with an increased annealing temperature.

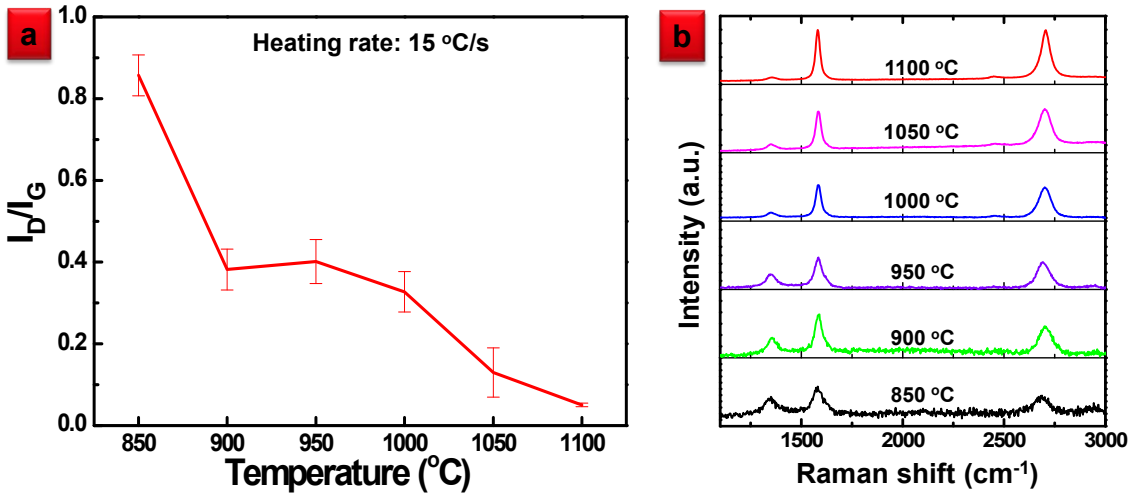

Fig. S3. Dependence of graphene quality on the RTP annealing temperature when the heating rate is set at 15 °C/s. (a) I_D/I_G ratio plot as a function of annealing temperature. (b) Corresponding Raman spectra under different annealing temperatures.

4. Theoretical calculation of Ni_3C decomposition temperature and carbon diffusion length as functions of RTP heating rate

a) *Calculation of Ni_3C decomposition temperature*

The mathematic model used for the calculation of Ni_3C decomposition as a function of the RTP heating rate was obtained from a previous study on Ni_3C thermal decomposition in argon (Ar) environments.[1] The equation is shown as follows:

$$\ln\left(\frac{R}{T_p^2}\right) = -\left(\frac{\Delta E}{K_B T_p}\right) + A \tag{1}$$

where, Tp is the Ni_3C decomposition peak temperature, R is the heating rate, ΔE is the activation energy for Ni_3C decomposition, K_B is the Boltzmann constant, and A is a constant.

Table S1. Experimental results of Ni_3C thermal decomposition[1]

Heating Rate, **R** (°C/min)	5	10	20
Ni_3C Decomposition Peak Temperature, **Tp** (°C)	400.15	415.05	424.85

Based on the Ni_3C decomposition experimental results, as shown in Table S1, the ΔE and A can be calculated as 204 kJ/mol and 15.4, respectively. Therefore, the relationship between Ni_3C decomposition peak temperature, Tp, and the heating rate, R, is established and is plotted in Fig. 5c.

b) *Calculation of carbon diffusion length*

Based on Fick's second law of diffusion, we have estimated the diffusion length of carbon during the RTP heating process. The mathematical model is shown in Equation 2.

$$L = 2\sqrt{\int_0^{t'} D(t)dt} \tag{2}$$

where, L is the carbon diffusion length, and D(t) is the carbon diffusion coefficient. According to previous experimental measurements on carbon diffusion,[2] the carbon diffusion coefficient in Ni can be derived as below:

$$D = D_0 exp(-E/K_B T) \quad (3)$$

$$T = 300 + Rt' \quad (4)$$

where, $D_0 \approx 0.1$ $cm^2 s^{-1}$, $E \approx 1.5$ eV, T is the environment temperature, R is the heating rate, and t' is the annealing time.

Based on the above Equations (2-4), we have calculated the carbon diffusion length before the beginning of Ni_3C decomposition (an onset Ni_3C decomposition temperature of 465 °C was used in this calculation). The plot of carbon diffusion length as a function of heating rate is shown in Fig. 5d.

5. Weight loss measurements in RTP process

We have measured the weight loss in the RTP process using microbalance. Table S2 shows the measurement result. It is shown that about 30% weight loss of the Ni/C thin film was observed after only 2 min RTP annealing process at 1100 °C. The weight loss experiments further confirm the evaporation of Ni_3C during the RTP annealing process.

Table S2. Weight loss measurement result.

Weight A: Before Ni/C deposition	**Weight B**: After Ni/C deposition	**Weight C**: After RTP annealing process	**Weight loss percentage** (Ni/C)
9.1610 g	9.1637 g	9.1629 g	29.6 %

6. Auger electron spectroscopy (AES) spectra of the compositional elements

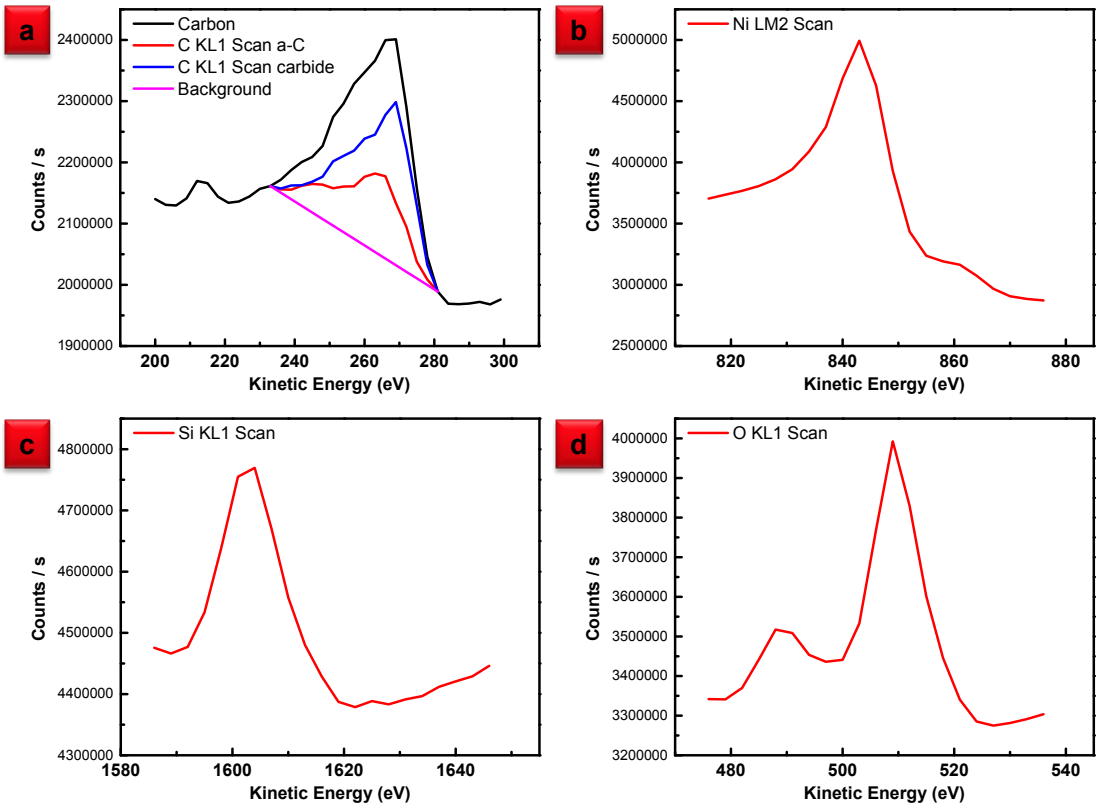

Fig. S4. Typical Auger electron spectroscopy (AES) spectra of each compositional elements including (a) Carbon, (b) Nickel, (c) Silicon, and (d) Oxygen during the AES depth profiling analyses of annealed Ni/C/SiO_2 samples.

Fig. S4 shows the typical AES spectra of the compositional elements in analyzing the Ni/C/SiO_2 samples. All the compositional elements have their characteristic AES peak positions and line shapes, enabling the quantitative analyses of the component concentrations in the AES depth profiling experiments. The peak fitting measures were obtained by the non-linear-least-square fitting software (Thermo, Microlab 310F).

References

1. Y. H. Leng, L. Xie, F. H. Liao, J. Zheng, X. G. Li, *Thermochimica Acta* **2008**, *473*, 14.

2. E.V.Rut'kov and N.R.Gall. Equilibrium Nucleation, Growth, and Thermal Stability of Graphene on Solids, Physics and Applications of Graphene - Experiments, Dr. Sergey Mikhailov (Ed.), ISBN: 978-953-307-217-3, InTech, **2011**.